Chapter 18
Strategies for Shaker Placement for Impedance-Matched Multi-Axis Testing

Daniel P. Rohe, Garrett D. Nelson, and Ryan A. Schultz

Abstract Multi-axis testing is growing in popularity in the testing community due to its ability to better match a complex three-dimensional excitation than a single-axis shaker test. However, with the ability to put a large number of shakers anywhere on the structure, the design space of such a test is enormous. This paper aims to investigate strategies for placement of shakers for a given test using a complex aerospace structure controlled to real environment data. Initially shakers are placed using engineering judgement, and this was found to perform reasonably well. To find shaker setups that improved upon engineering judgement, impact testing was performed at a large number of candidate excitation locations to generate frequency response functions that could be used to perform virtual control studies. In this way, a large number of shaker positions could be evaluated without needing to reposition the shakers each time. A brute force computation of all possible shaker setups was performed to find the set with the lowest error, but the computational cost of this approach is prohibitive for very large candidate shaker sets. Instead, an iterative approach was derived that found a suboptimal set that was nearly as good as the brute force calculation. Finally, an investigation into the number of shakers used for control was performed, which could help determine how many shakers might be necessary to perform a given test.

Keywords MIMO · IMMAT · Aerospace · Shaker · Excitation

18.1 Introduction

When a test article is operating in its service environment, it often experiences complex three-dimensional loading. However, when ground tests are performed, this complex environment is often reduced to a series of three uniaxial vibration tests. These uniaxial tests often do not accurately replicate the environment, especially considering that the test article must be bolted or otherwise attached to the shaker table, which can significantly alter the part's dynamics.

Impedance-Matched Multi-Axis Testing (IMMAT) is a technique that aims to improve the deficiencies in uniaxial vibration testing [1, 2]. IMMAT uses multiple smaller shakers to excite the structure, rather than a single large shaker. These smaller shakers allow spatially varying excitation in multiple directions simultaneously and additionally do not disrupt the boundary conditions of the test article as severely as when it is constrained in a vibration fixture on a large shaker. The IMMAT technique also attempts to match the boundary conditions of the test article in its service environment in order to allow the structure's dynamics to aid in meeting the environment (i.e. let the structure vibrate how it wants to vibrate). The key assumption is that if the responses of some set of control accelerometers are matched to the environment, the rest of the structure should also match the environment.

Often the data that can be obtained in a field environment test is limited. There are typically channel count limitations due to the necessity of an on-board data recorder. Due to the expense of performing environment tests in the field, the number

D. P. Rohe (✉) · G. D. Nelson · R. A. Schultz
Sandia National Laboratories, Albuquerque, NM, USA
e-mail: dprohe@sandia.gov

of iterations that can be performed to achieve good data is limited as well. For a ground test in the laboratory, many of these constraints are relaxed. A ground test can easily contain hundreds of channels; high-quality commercial data acquisition systems can be used, and instrumentation can be optimized for the specific portion of the environment that the ground test is examining. If a technique such as IMMAT can accurately reproduce an environment test on the ground, then many of the limitations of environment testing can be overcome.

One of the open questions regarding IMMAT is how to optimize shaker locations on the test article of interest. Often times for aerospace structures, the loading in service is provided by distributed aeroacoustic loads in addition to mechanical loads, which can make it difficult to intuitively reduce the service loading down to a handful of discrete force locations. With the goal of the IMMAT technique being to match the responses of control gauges in the laboratory test to those in the environment test, one important consideration is how well a given set of input locations can achieve the desired response. A second important consideration is how much force or power is required to achieve those responses, as larger shakers will take up more room around the test article and will require more infrastructure in terms of electrical power, voltage, and current as well as rigging and hoisting materials to support them. This paper aims to investigate shaker placement strategies for IMMAT on a realistic aerospace structure controlled to real environment data.

18.2 Test Hardware and Instrumentation

The structure of interest in this work is the bomb shown in Fig. 18.1. The structure was attached to a supporting rack. Soft bungee cords were used to support the rack. A frame was built up around the structure to create a flexible way to position shakers. During the environmental test, 21 channels of instrumentation were recorded, so for the ground test these instrumentation locations were reproduced. Nineteen of these channels were used for control, and two were used for validation. A number of additional channels of instrumentation were also placed on the exterior of the structure for extra diagnostics and potential drive point locations; however because there was no environment data for these locations, they could not be used for control during the laboratory test.

B+K Lan-XI data acquisition systems were used to record all channels of the laboratory test. These data acquisition systems can provide arbitrary source capabilities which were used in this test for open loop control. In addition, the control channels were teed off to a Spectral Dynamics Jaguar control system which provided closed loop control. The channels that were split were powered using external Kistler Piezotron Coupler signal conditioners.
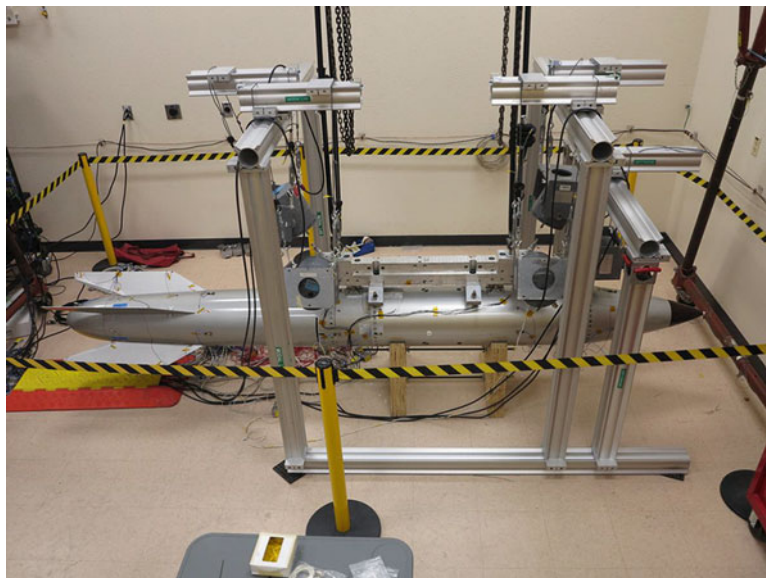
Fig. 18.1 Test Article with frame built for supporting shakers

18.3 What is a "Good" Test?

Prior to being able to make any kind of meaningful comparison between different shaker setups or control strategies, a suitable metric is needed that describes how well a test performed. For a single axis vibration test with one control accelerometer, such metrics can be derived easily; the power spectral density (PSD) function of the control accelerometer can be plotted against the target PSD, and a decibel (dB) error can be computed at each frequency line. The number of lines out of some tolerance can be counted, or an RMS dB error could be computed. For IMMAT this is more complicated. The single PSD curve in the single axis case becomes a complex-valued, square cross-power spectral density matrix, containing not only auto-power spectral density functions, but coherences and phases between the various control gages. This results in potentially hundreds of functions that could be compared between target and achieved responses. Clearly, some amount of data reduction is needed to be able to reduce this massive amount of data down to a more digestible metric.

In previous work on a similar structure, Mayes and Rohe used a "sum of autospectral densities" (ΣASD) metric to reduce the massive amount of data down to a single meaningful plot [3]. The metric used was the error in the sum of diagonal (trace) of the PSD matrix. Only the diagonals are considered, noting that the off-diagonal terms are strongly dependent on the dynamics of the individual test article and may vary between environment and ground tests. To compute the error metric, the dB error is computed between the target sum of ASDs and the actual response sum of ASDs. dB error was chosen due to the desire to compare relative magnitudes between control and achieved responses, rather than a linear error which would be biased towards the higher responding frequency lines.

This metric is shown in (18.1), where $G^t_{xx(i,i)}\left(f_j\right)$ and $G^e_{xx(i,i)}\left(f_j\right)$ denote the jth frequency line of the ith autospectrum (diagonal entry) for the test and environment data, respectively, and n_{gauge} is the number of control channels.

$$e_{\Sigma \text{ASD}}(f_j) = \text{dB}\left(\sum_{i=1}^{n_{gauge}}\left(G^t_{xx(i,i)}\left(f_j\right)\right)\right) - \text{dB}\left(\sum_{i=1}^{n_{gauge}}\left(G^e_{xx(i,i)}\left(f_j\right)\right)\right) \tag{18.1}$$

This can also be reduced to a single value by taking the RMS value of $e_{\Sigma \text{ASD}}(f_j)$ over all frequency lines, where n_{freq} is the number of frequency lines:

$$e_{\Sigma \text{ASD}} = \sqrt{\frac{1}{n_{freq}}\sum_{j=1}^{n_{freq}} e_{\Sigma \text{ASD}}(f_j)^2} \tag{18.2}$$

The error in the sum of the PSDs can give an estimate of the total energy in the system, but does not give a good estimate of the spatial distribution of that energy. The error in the sum of the PSDs may still be small even if the control is poor, because some gauge that is responding to a higher level than it should might make up for a gauge that is responding at a lower level than it should. A second metric considered in this work is an "RMS dB error" which calculates the dB error in the ASD for each gauge, and then calculates the RMS value over all gauges.

$$e_{\text{ASD}}(f_j) = \sqrt{\frac{1}{n_{gauge}}\sum_{i=1}^{n_{gauge}}\left(\text{dB}\left(G^t_{xx(i,i)}\left(f_j\right)\right) - \text{dB}\left(G^e_{xx(i,i)}\left(f_j\right)\right)\right)^2} \tag{18.3}$$

Like the previous metric, this can be rolled up into a single value by computing the RMS over all frequency lines:

$$e_{\text{ASD}} = \sqrt{\frac{1}{n_{freq}}\sum_{j=1}^{n_{freq}} e_{\text{ASD}}(f_j)^2} \tag{18.4}$$

This second e_{ASD} metric will be the primary metric used in this paper to determine whether or not a test is better or worse than another test. The $e_{\Sigma \text{ASD}}$ metric will also be presented for completeness and consistency with previous testing.

18.4 Control Strategies

While the focus of this paper is shaker placement optimization, it is helpful to understand the control schemes used for the testing described subsequently. Three different control schemes were utilized to control the response channels to the target responses; these are Uncorrelated Open Loop control, Closed Loop control, and Closed Loop Blended control, as described in the following sections. For all control strategies investigated, control channels 6 and 7 (shown on subsequent plots) were used for validation rather than control, allowing the authors to gain an understanding of what was going on at locations other than the control locations.

18.4.1 Uncorrelated Open Loop Control

An open loop uncorrelated (OL) control scheme was used successfully in [3], so it is used here as a starting point to compare against other more complex control schemes. The open loop scheme used in [3] computed shaker inputs using the pseudo-inverse of the transfer function matrix assuming uncorrelated inputs.

One issue with the approach in [3] is that there is no numerical constraint that the voltage autospectra remain positive, though this is a physical constraint. In the cases where the desired voltage autospectra were found to be negative, they were instead set to zero. This additional energy resulted in the responses of the control gauges being larger than the control specifications. Though the Tikhonov regularization reduced the incidences of negative energy being desired by the open loop control scheme, it could not completely eliminate them.

A non-negative least squares solver is available in MATLAB via the `lsqnonneg` function, which uses the algorithm from [4]. This algorithm solves the least squares problem with the constraint that the solution cannot be negative, effectively ensuring that physical voltage signals could be reproduced from the response. Using the non-negative least square solver produced better matches to the control accelerometers than the Tikhonov solution, so it was used for all open loop uncorrelated control.

In order to perform an open loop test, first a baseline "buzz" test was performed to establish the transfer functions. A pseudo-random signal was generated consisting of the summation of unit-amplitude sine waves at frequencies corresponding to the frequency bins of the Discrete Fourier Transform (DFT) with randomized phases for each frequency line for each frame. The signals were then scaled so they were 1/3 V RMS (approximately 1 V peaks) for each shaker. This signal was then fed through the shaker amplifiers by the arbitrary source capabilities of the B+K Lan-XI data acquisition systems, and the amplifier gains were adjusted to produce approximately 10 lbf RMS.

The MIMO transfer functions between the input voltage and output responses were computed from the baseline "buzz" test data. These transfer functions were then passed into the control equation and new voltage autospectra were computed via the non-negative least squares solution. The amplitudes of the baseline sinusoids were then scaled by the square root of the ratio between the new voltage autospectra and the old voltage autospectra, again with randomized phases to produce the updated input signal. This signal was then played by the arbitrary source capabilities of the B+K Lan-XI data acquisition systems and the responses to the control inputs were recorded.

18.4.2 Closed Loop Control

As a step up in complexity from the uncorrelated open loop control, a closed loop (CL) control scheme was attempted using the Spectral Dynamics Jaguar MIMO control system as described in Sect. 18.2. The Jaguar system attempts to solve the control equation directly without making assumptions on the inputs. This includes attempting to control to the off-diagonal entries of the PSD matrix, rather than discarding them to only match autospectra as was done in the Open Loop Uncorrelated control scheme. It does this by not only specifying the amplitudes of the voltage signals output to the shaker amplifiers, but also the phasing and coherence between the voltage signals.

18.4.3 Closed Loop Blended Control

While the nominal closed loop control described previously used both autospectra and crossspectra from the environment data, previous work [2] has suggested that better control can often be achieved by computing the cross-power spectral density

terms using the dynamics of the ground test structure rather than the environment test data. This so-called closed loop blended (CLB) approach uses as its control targets the diagonal of the PSD matrix from the environment test data but populates the off-diagonal terms of the target PSD matrix using the coherence and phase of the off-diagonals from a test performed at similar excitation level (typically from the closed loop control test). Attempting to control the off-diagonal terms to the environment data can be counter-productive due to differences in the dynamics between the environment test article and the ground test article; better control to the diagonal terms of the PSD matrix can be achieved if the ground test unit is allowed to vibrate in its preferred way.

To compute the coherence and phase, the response PSD matrix is taken from the closed loop control test. The coherence $\gamma^2_{(i,j)}$ and phase $\phi_{(i,j)}$ are computed for each (i, j) off-diagonal term in the PSD matrix as follows:

$$\gamma^2_{(i,j)} = \frac{\left|G_{xx(i,j)}\right|^2}{G_{xx(i,i)}G_{xx(j,j)}} \tag{18.5}$$

$$\phi_{(i,j)} = \arctan \frac{\mathrm{imag}\left(G_{xx(i,j)}\right)}{\mathrm{real}\left(G_{xx(i,j)}\right)} \tag{18.6}$$

Then the off-diagonal terms of the target environment PSD matrix are recomputed using the phase and coherence from the ground test and the diagonal terms of the target environment PSD matrix.

$$G_{xx(i,j)} = \sqrt{\gamma^2_{(i,j)}G_{xx(i,i)}G_{xx(j,j)}}e^{\hat{i}\phi_{(i,j)}} \tag{18.7}$$

With the blended PSDs created, they could be loaded into the Jaguar system as the control targets. The test would then proceed as described in Sect. 18.4.2.

18.5 Shaker Placement Strategies

Excitation locations have proven to be an important consideration for the IMMAT technique. This work aimed to investigate different shaker setups to see how shaker setup could be optimized in future tests. Initially shaker placement proceeded using engineering judgement, which has been shown to provide reasonable shaker locations [3]; however recent works have attempted to provide a more algorithmic or automatic approach. In [2] the authors developed modal approaches to positioning shakers while limiting the force required. For large, complicated aerospace structures such as the one in this test which may have hundreds of modes in the bandwidth of interest, a mode-based approach may not be feasible; there may be insufficient instrumentation available to fit all the modes in the bandwidth, and a finite element model from which modes could be extracted may not be accurate due to the complexity of the structure.

18.5.1 Engineering Judgement

The initial positions of the shakers in the test were decided upon using the previous test in [3] as a starting point and then modifying the shaker set based on engineering judgment. The shakers started in a configuration that closely matched the rack configuration from [3] with one shaker located on the tail. This configuration, shown schematically in Fig. 18.2, is called the Rack-Tail configuration in this report.

The second shaker configuration was created by moving the shakers from the rack to the bomb, which was also done in [3]. The tail shaker location from the Rack-Tail configuration was noted to improve control significantly, so a second shaker was added at this location perpendicular to the first tail shaker. The remaining three shakers were spaced along the length of the bomb. This configuration is shown in Fig. 18.3 and is hereafter called the Bomb shaker configuration.
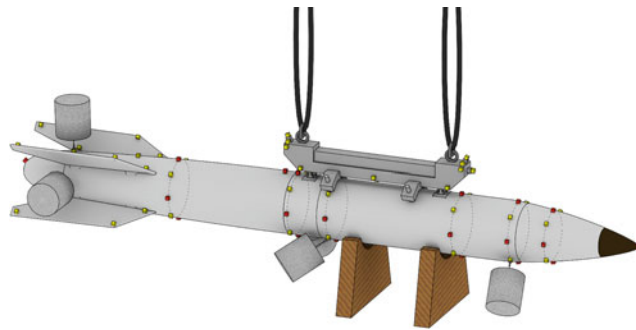
After testing the Bomb shaker configuration, it was noted that the axial control locations weren't responding accurately, likely because there is no significant axial shaker excitation. The Bomb configuration was modified such that the shaker at the middle of the bomb was rotated 45° to provide half axial/half radial excitation. This configuration is called Bomb2 and is
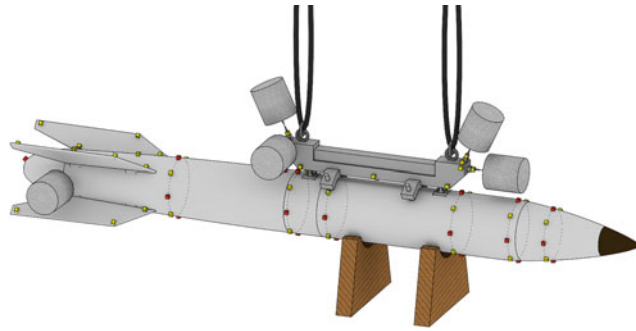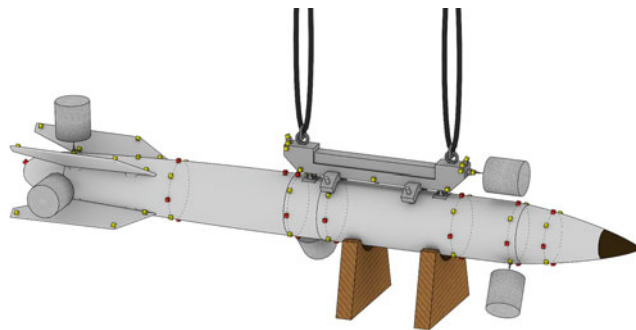
Fig. 18.2 Rack-Tail shaker configuration
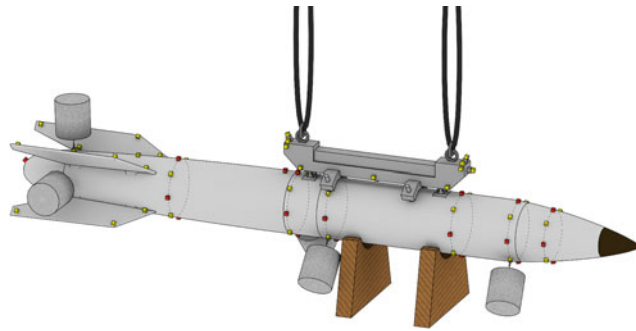
**Fig. 18.3** Bomb shaker configuration

Fig. 18.4 Bomb2 shaker configuration

Fig. 18.5 Rack-Bomb shaker configuration

shown in Fig. 18.4. Noting that the additional axial input improved the result, that shaker was moved to the axial location on the bomb rack to provide even better axial control. This configuration is called Rack-Bomb and is shown in Fig. 18.5. This configuration was considered the "best" configuration achieved using engineering judgment.
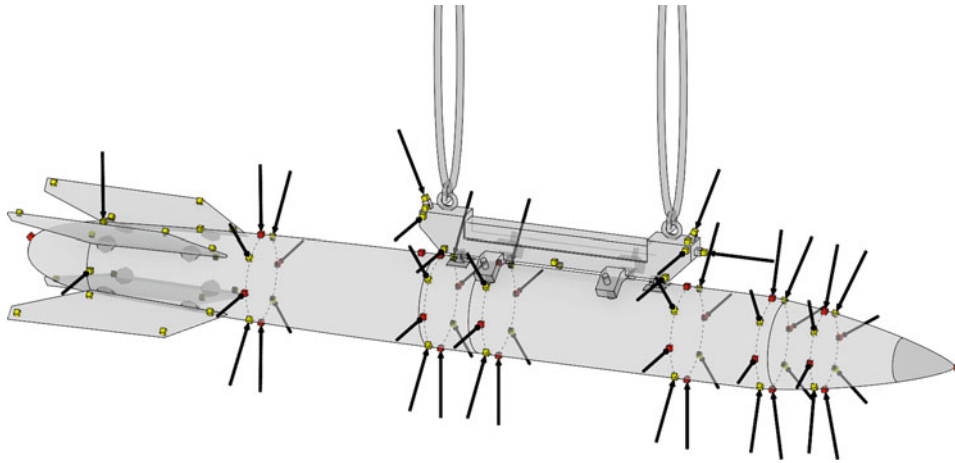
Fig. 18.6 Hammer impact locations to populate shaker candidate location transfer functions

18.5.2 Impact Testing to Populate the Transfer Function Matrix for Candidate Shaker Locations

The four shaker location sets described above were chosen based on engineering judgment and provided seemingly reasonable results. However, they are likely not the optimal set of shaker locations to provide the best results. Ideally, the test engineer would have some way of selecting a shaker setup that was optimal in some sense, rather than simply reacting to the results that are being achieved. For the investigation into optimal shaker setups, control was simulated analytically to try to find the best set of shaker locations. This allowed many shaker setups to be evaluated without spending the time repositioning the shakers between each evaluation.

Predictions of the response PSD matrices from a set of inputs can be computed via the control equation if a transfer function matrix is available for the candidate input locations. If a large number of columns (i.e. candidate input locations) are available, the test engineer can simply pick one of those columns for each shaker, run them through the control law analytically, and get estimates of the response to inputs at the locations corresponding to those five columns. The optimal input locations can then be selected as the five columns of the transfer function matrix that produced the best matches to the environment data. Setting up a large number of shakers to populate a large number of columns in the transfer function matrix can be time consuming due to the need to provide support for the shaker, align the stinger, and adhere the shaker hardware to the test article. An alternative to shaker excitation is hammer or impact excitation where an instrumented hammer can be used to excite the structure in more locations more quickly.

Impact hammer data was acquired at all external gauges on the body of the bomb where the bomb rack did not interfere with the impact testing (i.e. not on the fins or between the bomb rack and the bomb), as well as at six locations on the bomb rack for a total of 54 different input locations to populate candidate shaker locations. These impact locations are shown in Fig. 18.6. This set of locations contained all of the shaker locations used previously as described in Sect. 18.5.1, so the comparison between the responses predicted from Hammer transfer functions and actual shaker control responses could be performed.

18.5.3 Brute Force Computation of Minimum Error

It is straightforward to compute the estimated responses and compare them to the environment data for a set of shaker locations, so an attractive path forward might be to simply compute the responses for every combination of five shakers from the candidate set. With 54 candidate shaker locations, there are 3,162,510 unique combinations of five shakers, and the number grows quickly as more candidate locations are added. However, it was desired to simulate the control problem at each of these 3 million shaker setups to get an idea of the distribution of the error metrics and determine a true best shaker configuration against which other methods of shaker selection could be compared. The Closed Loop control scheme was chosen for this analysis over the Closed Loop Blended due to it being less computationally intensive; the Closed Loop Blended scheme requires two solutions of the control problem, the first to generate coherence and phase to update the off-
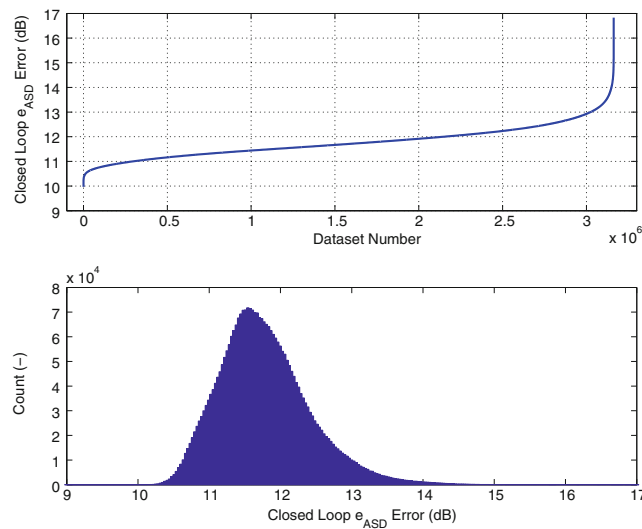
Fig. 18.7 Distribution of Error e_{ASD} for all 3,162,510 combinations of five shakers from 54 candidate locations
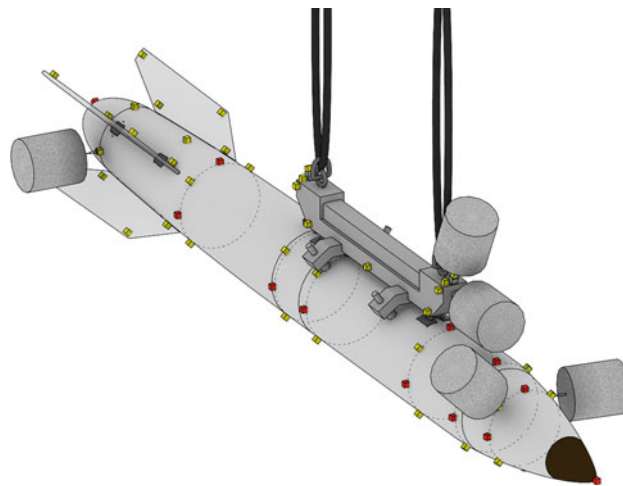
Fig. 18.8 Optimal Closed Loop shaker configuration showing two shakers on the rack and three on the bomb computed by brute force solution of all of the combinations of five shakers from 54 candidate shaker locations

diagonal terms of the target PSD matrix, and the second to compute the control to those updated targets. The Closed Loop control scheme only requires one solution of the control problem.

The Closed Loop computation of the full set of shaker input combinations was able to be performed on a laptop computer over approximately 36 h. The resulting error distribution is shown in Fig. 18.7. The distribution is skewed towards higher errors; there are many bad shaker locations, a large body of reasonable shaker locations, and a few good shaker locations. The shaker setup corresponding to the best Closed Loop prediction is shown schematically in Fig. 18.8 and will be referred to as the "Best Brute Force" shaker configuration. Unfortunately this configuration was unable to be set up in the laboratory due to the shaker trunnions, which are not shown in Fig. 18.8, interfering with adjacent shakers at the front of the rack; however, it is still useful as a comparison benchmark.

Note that there is a near-infinite number of candidate shaker locations on the bomb that could have been used so even this exhaustive search of the 54 candidate shaker locations may not select the *true* optimal shaker set as the locations that would provide such a set may not be included in the 54 candidate shaker locations.

The computational complexity of the brute force approach would grow exponentially if more candidate shaker locations were to be added, and would therefore not be feasible if, for example, a finite element model consisting of thousands of candidate locations were to be used to populate the full space of excitation locations. Therefore, a more computationally efficient method was desired to select a set of shakers from a potentially enormous candidate set.

18.5.4   Shaker Positioning by Iterative Addition of the Shaker that Minimizes Error

To provide an alternative to the brute force approach to compute a nearly optimal shaker set, a technique was derived that iteratively adds shakers that produce the minimum e_{ASD} error. Starting with zero shakers, the technique solves the Closed Loop Blended control problem with all candidate shaker locations individually, resulting in 54 response sets and 54 error metrics each derived using only a single shaker to excite the structure. The shaker that provides the lowest error is kept and the problem begins again except on the second iteration the shaker that was picked in the first iteration is combined with all remaining candidate shaker locations individually, resulting in 53 response sets and 53 error metrics each derived using two shaker locations. Again, the combination of two shakers that produces the lowest error metric is kept. The process continues until five shakers are selected. In total, only 260 solutions of the control problem are needed to perform this algorithm, rather than 3 million to exhaustively search the input space.

The shaker selection algorithm chose the configuration shown in Fig. 18.9. Note that this is not the same configuration selected by the best brute force calculation and is therefore suboptimal, though much more computationally efficient. The best single shaker was placed at the middle of the bomb in the lateral direction. This configuration also maintained the two tail shakers from the previous Bomb, Bomb2, and Rack-Bomb configurations. The final two shakers were placed on the nose, which provides the majority of the axial input for this configuration, and near where the aft bomb rack contacts the bomb. This configuration will be referred to as the "Bomb Suboptimal" shaker configuration. Because the shakers were reasonably spread out along the bomb, the configuration could be set up in the laboratory, and this is shown in Fig. 18.9b.

Control results for the four shaker configurations from Sect. 18.5.1 as well as the Bomb Suboptimal configuration are shown in Fig. 18.10, both for hammer predictions as well as laboratory results. It shows the control results from the laboratory test are predicted quite well by the impact hammer transfer functions, which validates the predictive ability of the hammer transfer functions.

18.5.5   Comparison of Shaker Selection Techniques

The shaker sets selected by the Closed Loop Brute Force and Iterative Shaker Addition algorithms were compared analytically against the Rack-Bomb setup, which was thought to be the best setup using engineering judgment, for the Open Loop, Closed Loop, and Closed Loop Blended control schemes, shown in Fig. 18.11. One interesting point that can be seen in Fig. 18.11 is that the best shaker setup for one control scheme is not necessarily the best for other control schemes. For example, the Bomb Suboptimal shaker set performed better than the Best Brute Force shaker set for the Open Loop control, significantly worse for the Closed Loop control, and only slightly worse for the Closed Loop Blended.

This is an interesting point because the brute force calculation showed the Bomb Suboptimal shaker setup selected by the Iterative Shaker Addition algorithm was only in the top 1.5% of shaker setups, with over 45,000 of the 3 million candidate shaker setups performing better; however this brute force computation was performed using the Closed Loop control scheme rather than the Closed Loop Blended control scheme. It appears that the Bomb Suboptimal shaker setup would have performed much closer to the Best Brute Force setup had the Closed Loop Blended control scheme been used in the brute force computation.

To further investigate this phenomenon, the responses from the Open Loop, Closed Loop, and Closed Loop Blended control problems were predicted using hammer impact data for 15,000 random shaker sets of five shakers from the 54 candidate locations shown in Fig. 18.6 and compared against those shaker sets that have been described previously. Figure 18.12 shows histograms of the errors from the 15,000 samples for the three shaker control schemes, with the positions of the Rack-Tail, Bomb, Bomb2, Rack-Bomb, Bomb Suboptimal, and Best Brute Force shaker configurations labeled. The distribution of each control scheme's errors was again skewed towards larger errors. Another way to look at the distributions is shown in Fig. 18.13, which sorts the datasets by increasing error.

To get an idea of how well error in one control scheme correlated to error in another control scheme, the predicted errors were compared between control schemes for individual shaker sets. Figure 18.14 shows these results. The Rack-Tail, Bomb, Bomb2, Rack-Bomb, Bomb Suboptimal, and Best Brute Force shaker setups are also marked on the plots so one can see how well they performed compared to other shaker sets. It is obvious from these plots that there is a difference between performance of a given shaker configuration between control schemes. For example, the Rack-Tail configuration, which performed rather poorly compared to other shaker setups in the Open Loop case actually performed quite well in the Closed Loop and Closed Loop Blended cases. And while there were many shaker configurations found to be better than the Bomb Suboptimal setup in the Closed Loop case (over 45,000 different combinations or 1.5% per the brute force analysis), in the
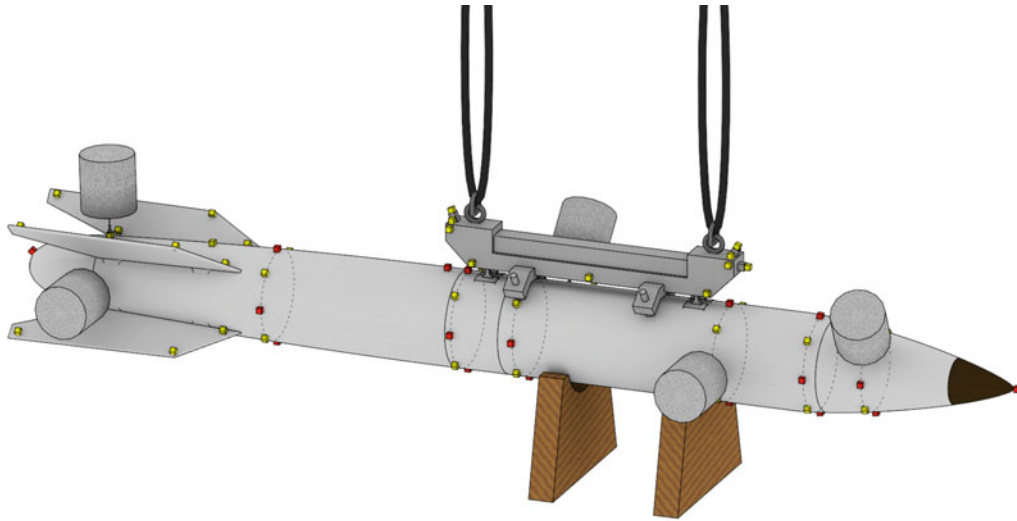
(a)
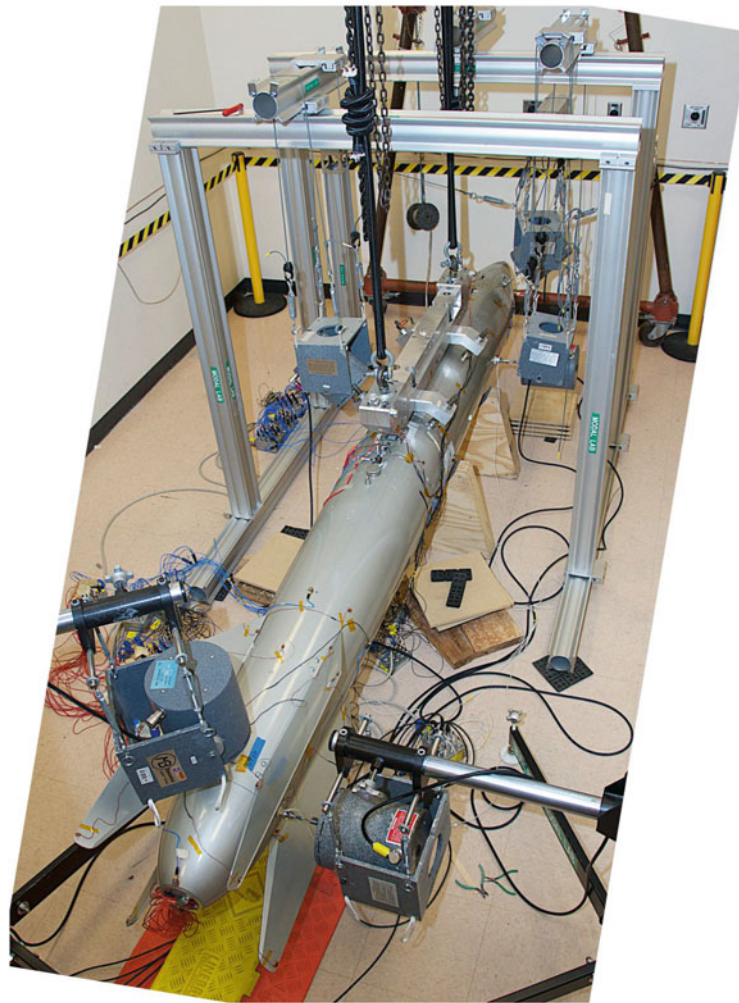
(b)

Fig. 18.9 Suboptimal shaker configuration showing all five shakers located on the bomb. (**a**) Schematic view. (**b**) Test article with shakers attached
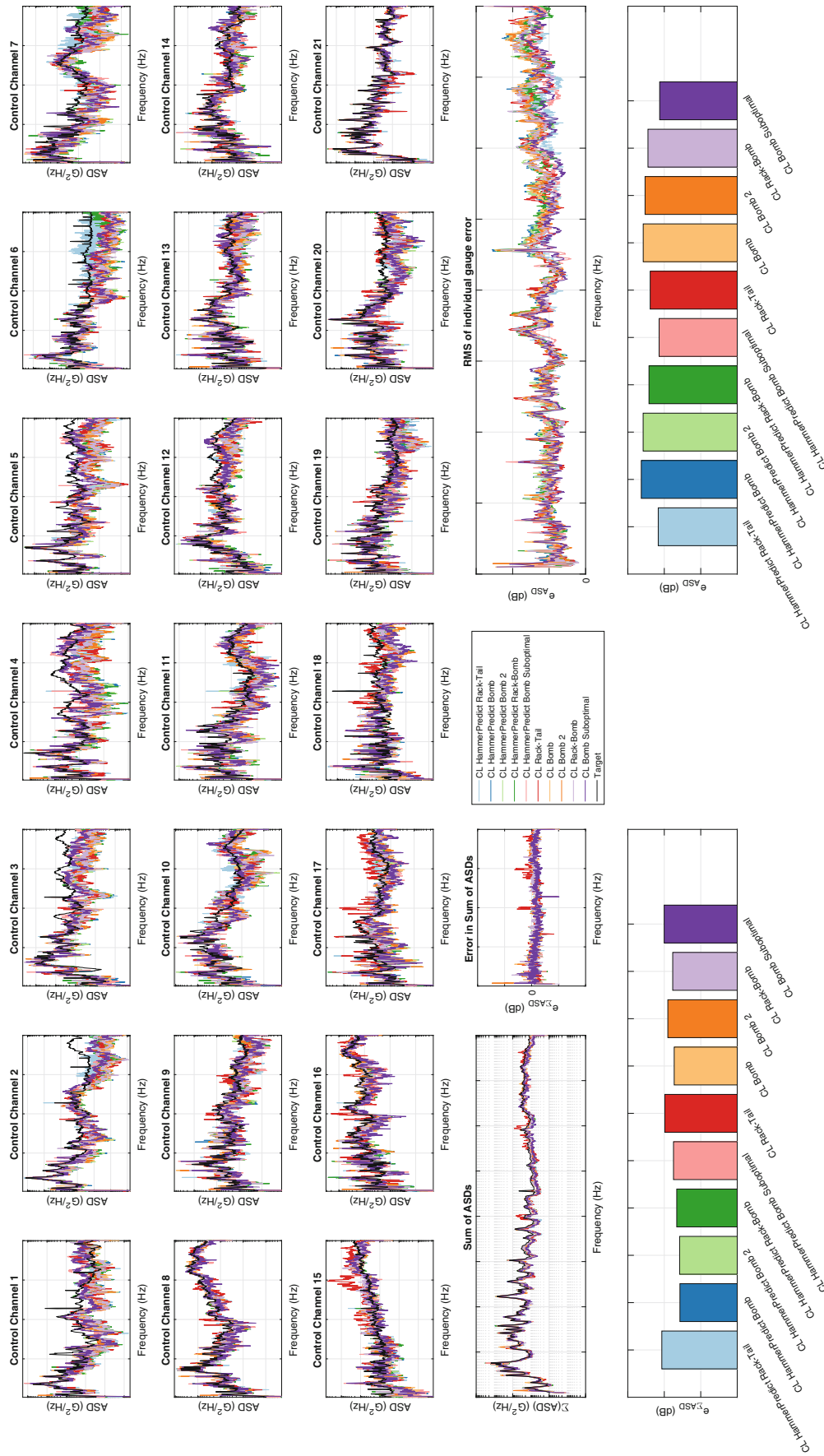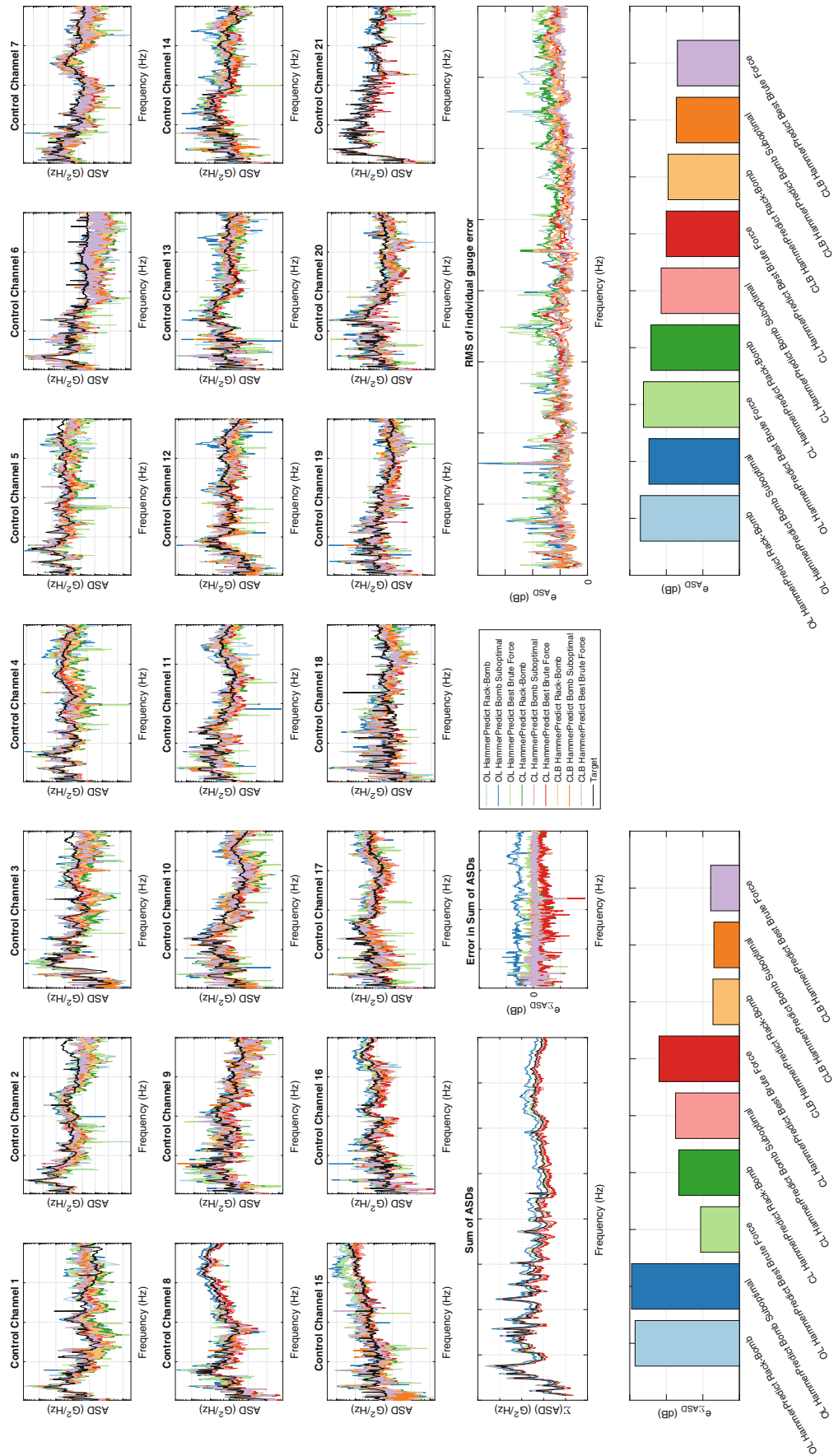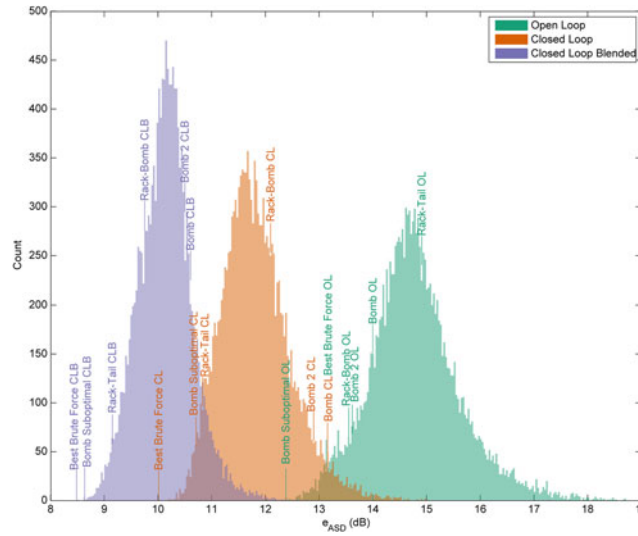
Fig. 18.10 Validation of hammer predictions showing that the predicted Bomb Suboptimal error was actually achieved in the laboratory

Fig. 18.11 Predicted control for the Rack-Bomb, Bomb Suboptimal, and Best Brute Force configurations for Open Loop, Closed Loop, and Closed Loop Blended shaker control strategies

Fig. 18.12 Histogram of e_{ASD} errors for 15,000 random shaker sets for Open Loop, Closed Loop, and Closed Loop Blended control schemes. Specific shaker setups discussed previously are marked on each histogram
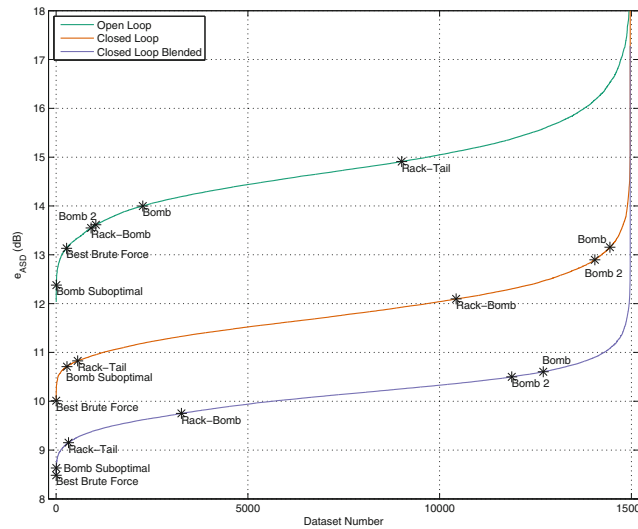
Fig. 18.13 Shaker setups sorted by increasing error for Open Loop, Closed Loop, and Closed Loop Blended control schemes for 15,000 shaker setups. Specific shaker setups discussed previously are marked on each curve

Closed Loop Blended case it was very nearly the best shaker setup found (only the Best Brute Force shaker setup was found to be better). The Open Loop control scheme generally performed worse than the Closed Loop control scheme; however one shaker setup was found that performed better in the Open Loop control than in the Closed Loop control. This can be seen in Fig. 18.14a where a single point is above the diagonal green line that designates equal errors between the two control schemes.

The comparison between the Closed Loop and Closed Loop Blended control schemes in Fig. 18.14c showed the best correlation with the least amount of spread from the line of best fit. This suggests that it might be allowable to perform the computationally simpler Closed Loop control scheme to predict the best shaker setup, whereas performing the shaker optimization using an Open Loop control scheme might be less likely to produce a good Closed Loop Blended shaker setup. This is consistent with the Best Brute Force shaker setup computed from Closed Loop predictions also having the best Closed Loop Blended response out of all the shaker configurations checked, though it is possible that there is a better setup that simply has not been found as only 0.5% of the configurations were checked.
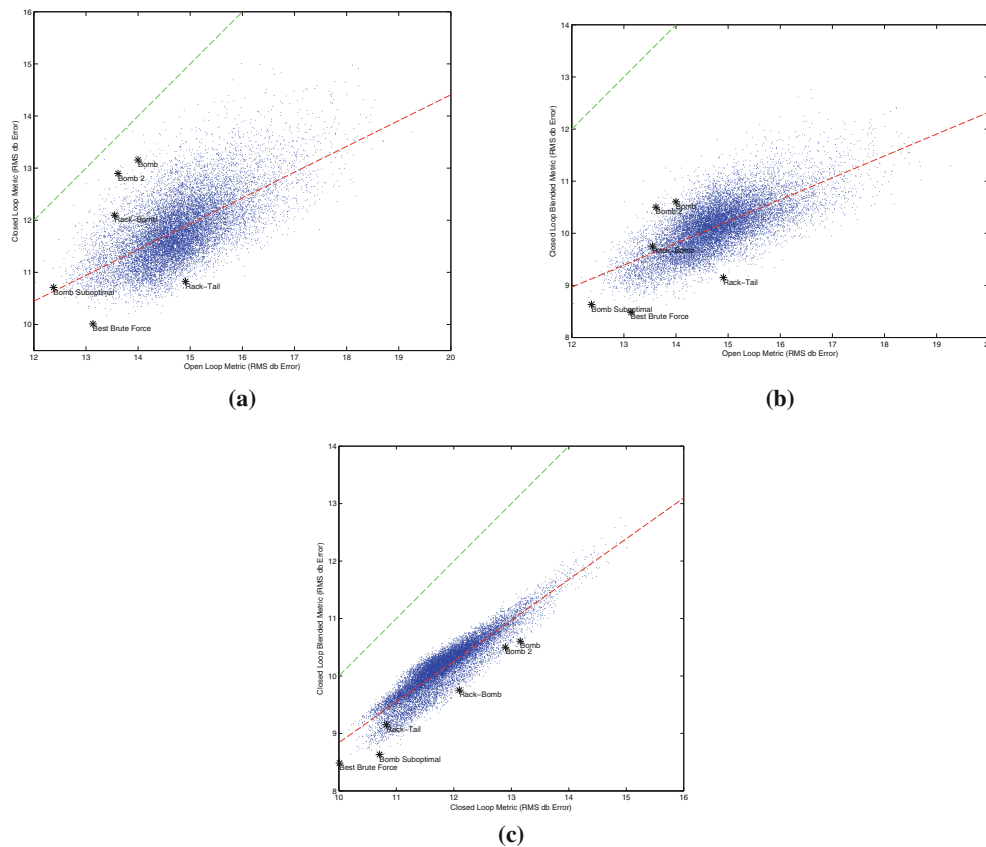
Fig. 18.14 Comparisons of Errors Between Control Schemes for 15,000 shaker setups. (**a**) Comparison between Open Loop and Closed Loop error. (**b**) Comparison between Open Loop and Closed Loop Blended error. (**c**) Comparison between Closed Loop and Closed Loop Blended error

### 18.5.6 Discussion of Number of Shakers Used for Control

In addition to the positions of the shakers, the number of shakers is also a parameter that the test engineer can control. Of particular interest is how the control and forces required change as shakers are added or removed. The Iterative Shaker Addition algorithm was again solved on the 54 candidate shaker locations; however instead of stopping after five shakers, the algorithm was allowed to run until 30 shakers were added. Recalling that there were 21 internal instrumentation channels, of which only 19 were used for control, the addition of the 19th shaker created a square control problem that is theoretically exactly solvable, and additional shakers past the 19th turn the rectangular "least-squares" solution where there is no exact solution (only a "best fit" solution) into a "underdetermined" or "minimum norm" solution where there are infinitely many solutions but only one that produces a minimum norm of the input. Note that because the Iterative Shaker Addition algorithm adds shakers based on the one that produces the minimum error, and the error is theoretically zero (though practically is some small number), it isn't clear that additional shakers added after the problem becomes square are in any way optimal or if they are based on small floating point errors. They could potentially be optimal in the sense that there may be larger floating point errors in the case where the matrix is more ill-conditioned, and thus the algorithm should pick the shaker that produces the best conditioned transfer function matrix, but further investigation is necessary prior to making that claim.

Figure 18.15 shows the effect of continually adding shakers on the control gauges and validation gauges (channels 6 and 7). The errors in the control gauges trend towards zero and are approximately zero when the control problem becomes square at 19 shakers. As more shakers are added, the approximately zero error slightly decreases likely due to an improving condition number on the transfer function matrix resulting in smaller numerical errors. If one examines only the response gauges used in the control process, it would appear that performing square control would be optimal; nearly perfect control is achieved using the minimum number of shakers. However there are a number of problems when the control problem becomes square.

Figure 18.16 plots the condition number of the transfer function matrix against the number of shakers in the control problem. The condition number is at its worst for a square problem and decreases as columns are added or removed.
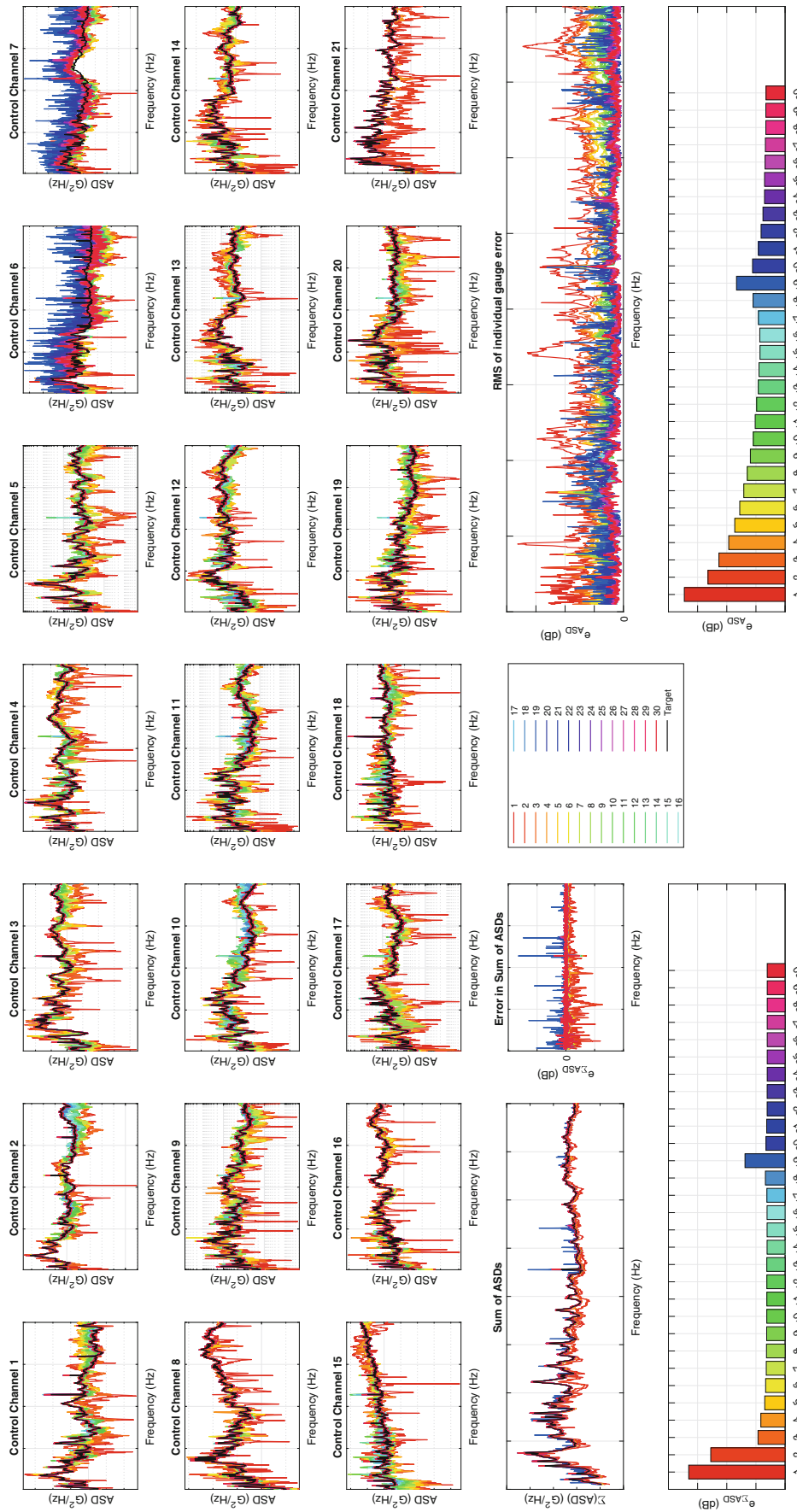
Fig. 18.15 Comparison of control for varying number of shakers. The top three rows of plots show the autospectral density functions for each control gauge, and how well the individual control strategies matched. The two plots in the fourth row show the dB error in the sum of the autospectral density functions ($e_{\Sigma ASD}$ from Eq. (18.1)) and the dB error in the autospectral density (e_{ASD} from Eq. (18.3)) at each frequency line. The bottom two plots show the same error metrics over all frequency lines
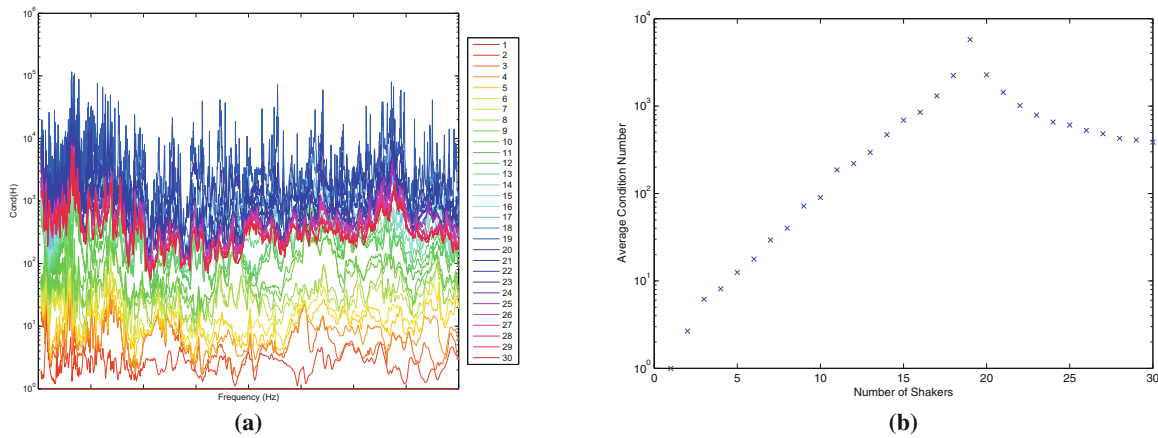
Fig. 18.16 Condition number of the transfer function matrix as the number of shakers is varied. (**a**) Condition number of the transfer function matrix for each frequency as the number as shakers is increased. (**b**) Average condition number of the transfer function matrix as the number as shakers is increased
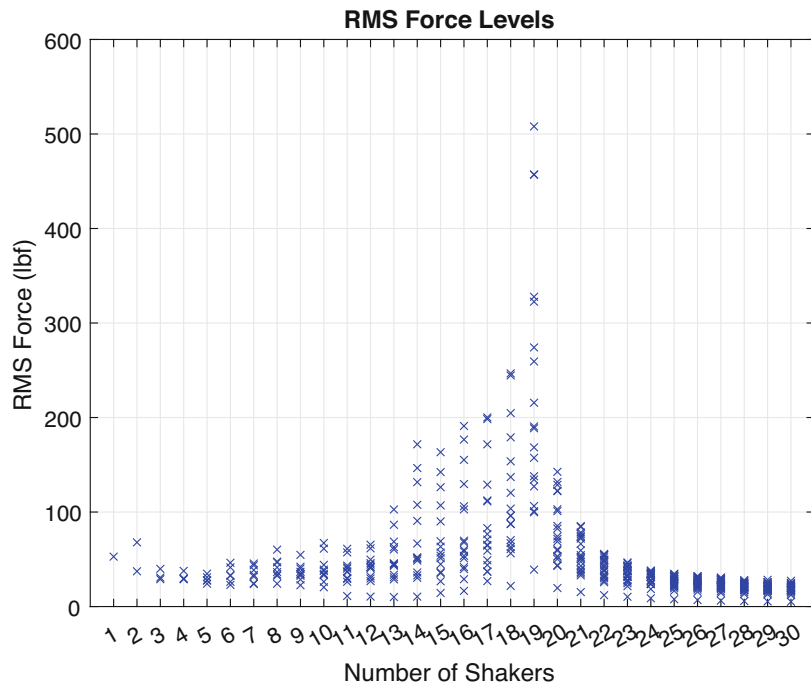
Fig. 18.17 RMS forces predicted to achieve control with an increasing number of shakers

Physically, a large condition number means that in order to achieve a small change in the responses, a large change in the input forces is required. This can be seen clearly in Fig. 18.17, which plots the RMS forces required to achieve the control. There is a clear maximum in the forces required at square control. One might expect that the force required should decrease with the number of shakers because the shakers can work together, and indeed this would be the case if the same number of control channels were used (i.e. split one control voltage to multiple shakers). However, the addition of extra control degrees of freedom gives the shakers more opportunity to fight against each other to achieve better control. Once past the point of square control, the solution to the control problem becomes a minimum norm solution that quickly reduces the maximum force required. Adding just one more shaker brings the maximum required force from 180 pounds RMS to approximately 50 pounds RMS, and continuing to add shakers results in further reduction in force.

Even if large shakers are available so that force is not a limiting factor in the test setup, performing square control is not advisable. While the control points are forced to exactly match the targets, the rest of the test article will not match as well. This can be seen by examining the validation channels, shown in Fig. 18.18. The error in the validation channels, shown in
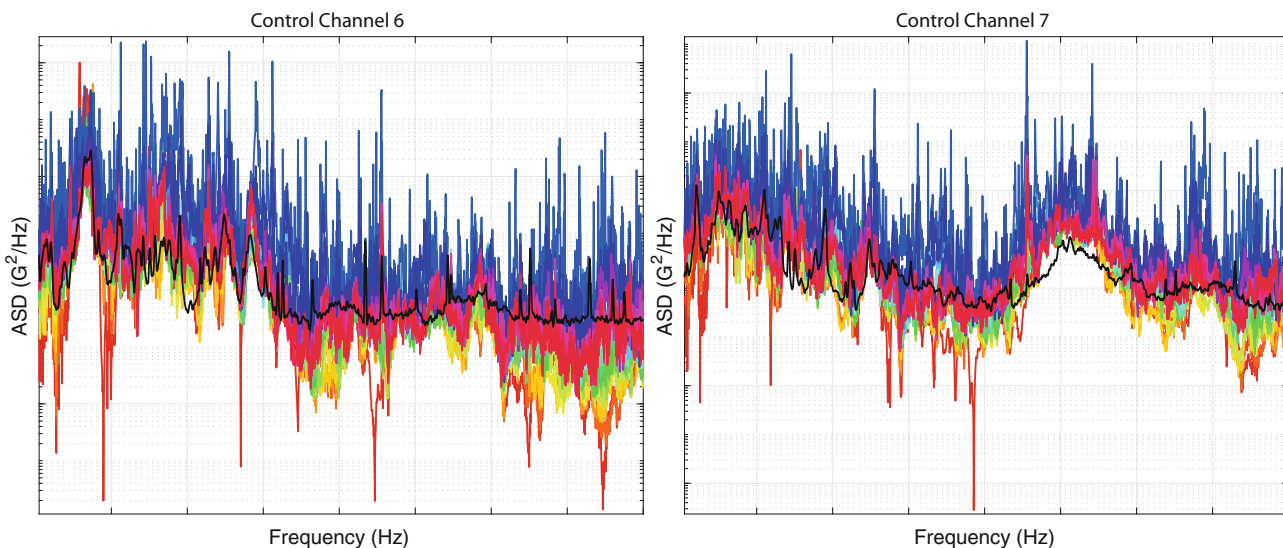
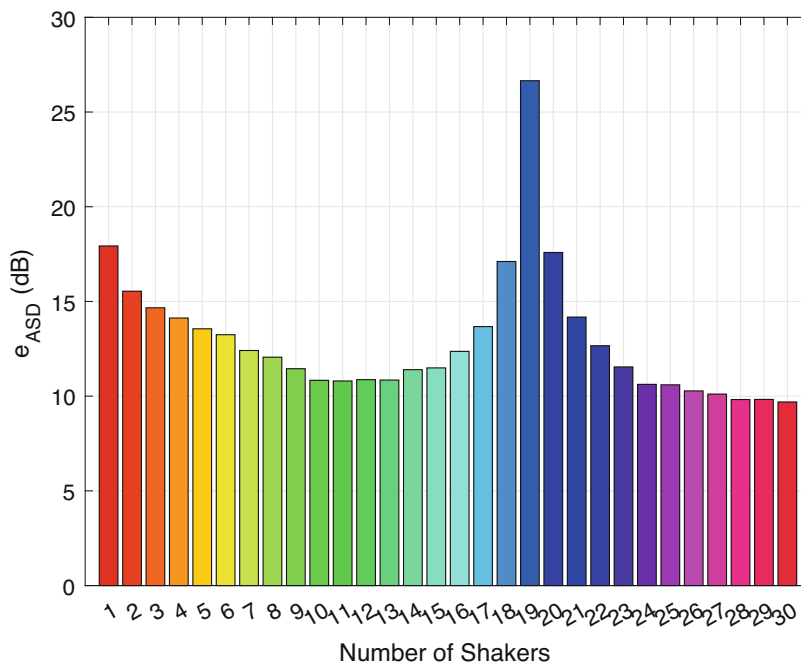**Fig. 18.18** Responses at the validation channels

Fig. 18.19 RMS dB error (e_{ASD}) from only the validation channels (6 and 7)

Fig. 18.19, reaches a local minimum at 10 or 11 shakers, but then proceeds to grow to a very large value when the problem becomes square. The responses at the validation channels are much too high in the square problem. As more shakers are added the responses return to reasonable values and the error again decreases.

18.6   Conclusions

In order to perform comparisons between control strategies and shaker setups, a suitable metric to determine which test is "better" in some sense is required. In a single-axis shaker test with a single control accelerometer, it can be straightforward to determine how well a test met the specifications; with a single PSD to compare, metrics like dB error and number of frequency

lines outside of some tolerance are commonly used. However, for a MIMO control problem as is found in IMMAT, it can be more difficult to determine a metric that describes how good the test was. This work has characterized all testing performed in terms of two metrics, both focusing on the diagonal terms of the PSD matrix. The RMS dB error, e_{ASD}, seemed to be the better indicator of a good test in this work, though future work in this area would certainly be of value.

In terms of shaker positioning, engineering judgment seems to have selected reasonable shaker setups in the middle of the error distributions. The best shaker setup for a given test was found to be dependent on the control strategy used. As moving the shakers to different positions was a time-intensive task, shaker setups were instead examined computationally using transfer function matrices derived from impact tests using an instrumented modal hammer. These proved to be a good tool for examining candidate shaker setups, though in a more nonlinear test structure the hammer force to control response transfer functions may not match as well to the transfer functions that would be obtained in a high-level shaker test. For this test, however, many shaker setups could be quickly evaluated by populating a transfer function matrix from a combination of hammer test transfer functions. A finite element model could be another method to develop force to control gauge transfer functions. If large computational resources are available, the control problem could be solved for all combinations of input locations in a brute force way, selecting the true optimal shaker configuration from the candidate locations available. The computations are also easily parallelized by splitting the candidate shaker combinations over multiple processors. If brute forcing a solution is too computationally intensive, the Iterative Shaker Addition Algorithm technique provided a very good, though suboptimal, solution to shaker positioning for this test.

A smaller error on the control gauge responses does not necessarily indicate a better test, as was shown in the analysis of number of shakers. The key assumption of IMMAT is that the entire structure behaves as it does in an environment if the control gauges are behaving as they do in the environment. While nearly zero error can be obtained on the control gauges autopower spectral density functions if the number of shakers is equivalent to the number of control gauges, it was found that the rest of the structure was actually performing less like it was in the environment than when only one shaker was used (which might be similar to the results obtained in a uniaxial shaker test). Practically, one may not be able to use 19 shakers on a single test, so the problem with square control might not be very applicable in this case, but this is an important consideration when performing this technique on structures where a smaller number of control gauges are available.

The optimum number of shakers to best match the validation gauges in this test was found to be 11, which is a bit more than half the number of control gauges. Alternatively, if a very large number of shakers could be used (30+), it would seem from this analysis that the error could be similarly reduced. Again, using one and a half times the number of shakers as control gauges may not seem practical for 19 control channels, but it may be for tests where there are a smaller number of control channels. Also of interest is the fact that when using a number of shakers larger than the number of control gauges the required force drops off fairly rapidly, so smaller, less-expensive shakers could potentially be used.

References

1. Daborn, P., Ind, P., Ewins, D.: Enhanced ground-based vibration testing for aerodynamic environments. Mech. Syst. Sig. Process. **49**(1), 165–180 (2014)
2. Daborn, P.M.: Scaling up of the impedance-matched multi-axis test (IMMAT) technique. In: Harvie, J.M., Baqersad, J. (eds.) Shock & Vibration, Aircraft/Aerospace, Energy Harvesting, Acoustics & Optics, vol. 9, Conference Proceedings of the Society for Experimental Mechanics Series, pp. 1–10. Springer, Cham (2017)
3. Mayes, R.L., Rohe, D.P.: Physical vibration simulation of an acoustic environment with six shakers on an industrial structure. In: Brandt, A., Singhal, R. (eds.) Shock & Vibration, Aircraft/Aerospace, Energy Harvesting, Acoustics & Optics, vol. 9, Conference Proceedings of the Society for Experimental Mechanics Series, pp. 29–41. Springer, Cham (2016)
4. Lawson, C.L., Hanson, R.J.: Solving Least-Squares Problems, chap. 23, p. 161. Prentice Hall, Upper Saddle River (1974)